IIETA International Information and Engineering Technology Association
Advancing the World of Information and Engineering

Annales de Chimie - Science des Matériaux
Vol. 50, No. 1, February, 2026, pp. 33-42
Journal homepage: http://iieta.org/journals/acsm

Effect of Calcium Carbonate on Mechanical and Thermal Properties of 3D-Printed PLA Honeycomb Sandwich Composites

Teguh Prasetyo[1*], Mirza Pramudia[1], Mahrus Khoirul Umami[1], Kusmono[2], Muhammad Syaiful Fadly[3], Binsar Maruli Tua Pakpahan[4]

[1] Department of Industrial and Mechanical Engineering, Universitas Trunojoyo Madura, Bangkalan 69162, Indonesia
[2] Department of Mechanical and Industrial Engineering, Universitas Gadjah Mada, Yogyakarta 55281, Indonesia
[3] Department of Mechanical Engineering, Universitas Tadulako, Palu 94118, Indonesia
[4] Department of Mechanical Engineering, Universitas Negeri Medan, Medan 20221, Indonesia

Corresponding Author Email: teguh.prasetyo@trunojoyo.ac.id

Copyright: ©2026 The authors. This article is published by IIETA and is licensed under the CC BY 4.0 license (http://creativecommons.org/licenses/by/4.0/).

https://doi.org/10.18280/acsm.500104

Received: 28 November 2025
Revised: 6 February 2026
Accepted: 16 February 2026
Available online: 28 February 2026

Keywords:
sandwich composite, additive manufacturing, calcium carbonate, mechanical properties, thermal stability

ABSTRACT

The development of lightweight structural materials with superior mechanical performance has driven the use of sandwich composites manufactured via additive manufacturing (AM). This study aims to analyze the effect of calcium carbonate ($CaCO_3$) weight fraction variation on the mechanical properties (tensile and flexural tests) and thermal stability (Thermogravimetric Analysis) of honeycomb-core sandwich composites with glass fiber skins fabricated using additive manufacturing and hand lay-up methods, with $CaCO_3$ contents of 0, 5, 10, and 15 wt%. The test results indicate that the tensile strengths were 48.612 MPa, 49.082 MPa, 45.625 MPa, and 36.585 MPa, respectively, while the corresponding flexural strengths were 76.486 MPa, 78.647 MPa, 66.046 MPa, and 43.432 MPa for 0, 5, 10, and 15 wt% $CaCO_3$. An improvement in mechanical strength was observed at 5 wt% $CaCO_3$ addition; however, a significant decline occurred at filler contents ≥ 10 wt%. Morphological observations using SEM revealed particle agglomeration at 10 wt%, which reduced mechanical strength by increasing stress concentration and weakening interfacial bonding. Meanwhile, Thermogravimetric Analysis (TGA) results demonstrated that the incorporation of $CaCO_3$ increased the onset temperature (T_{onset}) and maximum degradation temperature (T_{max}), indicating enhanced thermal stability of the composite.

1. INTRODUCTION

Three-dimensional (3D) printing, also known as additive manufacturing (AM) has attracted significant attention from industry over the past few decades. This growing enthusiasm has fueled expectations for the development and commercialization of materials compatible with a range of AM techniques. The innovation has been progressively adopted and is now used in the production of products and components across multiple sectors, including aerospace, medical, automotive, and even off-site construction [1, 2]. The implementation of AM technology in off-site construction has the potential to enhance overall efficiency throughout the construction process stage [3, 4]. AM is a free-form fabrication technique based on solid materials that produces objects layer by layer from a computer-based 3D geometric model, without requiring molds or tooling. Consequently, this process is not constrained by the limitations typically encountered in conventional manufacturing methods such as casting, forging, or machining. AM also has substantial potential to reduce energy consumption in manufacturing by minimizing material waste and eliminating secondary machining. Several studies have suggested that the widespread adoption of AM could significantly reduce global energy demand, potentially by up to 27% [5, 6].

One of the promising applications of AM technology is the fabrication of sandwich composite panels for structural elements in the construction sector, particularly through the printing of complex honeycomb core geometries. Sandwich composites are fabricated by bonding two high-strength face sheets to a lightweight core, resulting in structures with excellent strength-to-weight ratios [7, 8]. This configuration provides a combination of high strength and stiffness with low mass, enabling superior flexural performance, improved buckling resistance, and enhanced energy absorption under impact loading. Mechanically, the face sheets carry the majority of the applied load, while the core provides continuous support to stabilize the skins [9, 10]. Therefore, the core must possess low density while maintaining sufficient thickness to increase flexural rigidity and prevent buckling [11, 12]. Several studies have demonstrated that the physical and mechanical characteristics of sandwich composites are strongly influenced by the properties of the face sheets and the quality of the interfacial bonding between the skin and the core [13]. One approach to enhancing both performance and interfacial bonding in polymer-based sandwich composites is

the incorporation of inorganic fillers, such as calcium carbonate ($CaCO_3$) [14, 15].

Previous research has shown that adding $CaCO_3$ powder as a filler to composite materials can improve mechanical and thermal properties, including increased hardness [16], compressive strength [17], tensile strength, thermal resistance, and reduced microcrack formation within the matrix [18]. Furthermore, $CaCO_3$ can enhance matrix–fiber interfacial bonding, thereby improving fracture toughness and flexural strength [19, 20] and thermal stability [21]. However, several studies have also reported that excessive $CaCO_3$ content can reduce tensile strength, strain, elastic modulus, flexural strength, and impact strength. This decline is primarily due to particle agglomeration, in which fine particles cluster to form larger aggregates, leading to non-uniform dispersion within the matrix. At certain $CaCO_3$ concentrations, a larger portion of the composite surface becomes dominated by particle–polymer contacts [22, 23]. Such interfaces typically exhibit lower bonding strength compared to polymer chain interactions, thereby acting as weak zones that facilitate deformation under mechanical loading [24, 25].

This study aims to evaluate the effect of $CaCO_3$ volume fraction on the properties of sandwich composites fabricated via the hand lay-up method, incorporating a 3D-printed PLA honeycomb core and fiberglass skins. The addition of $CaCO_3$ is expected to significantly enhance the mechanical performance and thermal stability of the composite, thereby optimizing its overall structural performance. This improvement is particularly crucial for sandwich panel applications in the construction sector, where materials are required to possess high strength, adequate stiffness, lightweight characteristics, and resistance to mechanical loading and temperature fluctuations [19, 26]. Therefore, this research is expected to make a scientific contribution to the development of more efficient and adaptable sandwich composites that meet the demands of modern engineering applications.

2. EXPERIMENTAL WORK

2.1 Materials preparation

This study utilizes glass fiber with random orientation as the skin (Figure 1) and epoxy resin as the matrix. The core material is produced via 3D printing with an environmentally friendly PLA polymer filament (Sunlu brand, 1.75 mm diameter). The core features a honeycomb pattern, with printing parameters and geometric configurations presented in Figure 2, and is filled with $CaCO_3$ powder with a mesh size of 200.

Figure 1. Fiberglass chopped strand mat

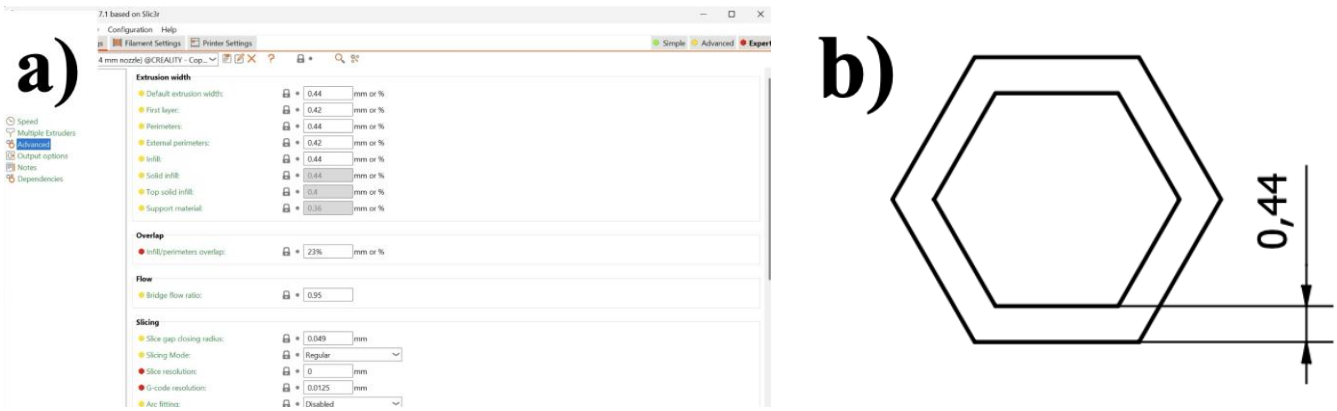

Figure 2. Honeycomb core fabrication (a) Honeycomb core printing parameters, (b) Honeycomb pattern geometry

2.2 Manufacturing of the honeycomb core

The honeycomb core was fabricated using a Creality Ender 3 Pro 3D printer. The printing performance parameters are presented in Table 1, while the honeycomb core printing process is illustrated in Figure 3.

2.3 Fabrication of tensile and flexural test specimens

The tensile test specimens were prepared in accordance with ASTM D3039, while the flexural test specimens followed the ASTM D790-03 standard. In this study, the epoxy matrix, serving as the bonding layer, was modified by incorporating $CaCO_3$ powder at 0, 5, 10, and 15 wt%. The process began with the fabrication of the honeycomb core using Fused Deposition Modeling (FDM) technology. Subsequently, the epoxy resin and $CaCO_3$ powder were mixed thoroughly to ensure homogeneous dispersion of the $CaCO_3$ particles within the matrix. The sandwich panels were fabricated by first impregnating the fiberglass bottom skin with the modified

resin, then placing the honeycomb core on top. The upper skin layer was then added, and the laminate was consolidated using a roller to minimize void formation and improve interfacial bonding quality. The fabricated sandwich composite panels were then conditioned at room temperature for 24 hours to allow curing, enabling optimal cross-linking and enhancing the material's mechanical stability. The configuration of the sandwich composite structure is illustrated in Figure 4.

2.4 Tensile and flexural testing

The sandwich composite specimens fabricated using the hand lay-up process were subsequently subjected to tensile and flexural tests using a Universal Testing Machine (UTM), SHIMADZU AGX-V2, with a maximum loading capacity of 50 kN and a controlled crosshead speed of 1 mm/min. The schematic diagrams of the tensile and flexural test setups are shown in Figure 5.

Table 1. 3D printing parameters

Printing Parameter	Value
Filament	PLA
Infill pattern	Honeycomb
Nozzle temperature	220 °C
Printing speed	35 mm/s
Bed temperature	60 °C
Infill density	60%
Layer thickness	0.2 mm

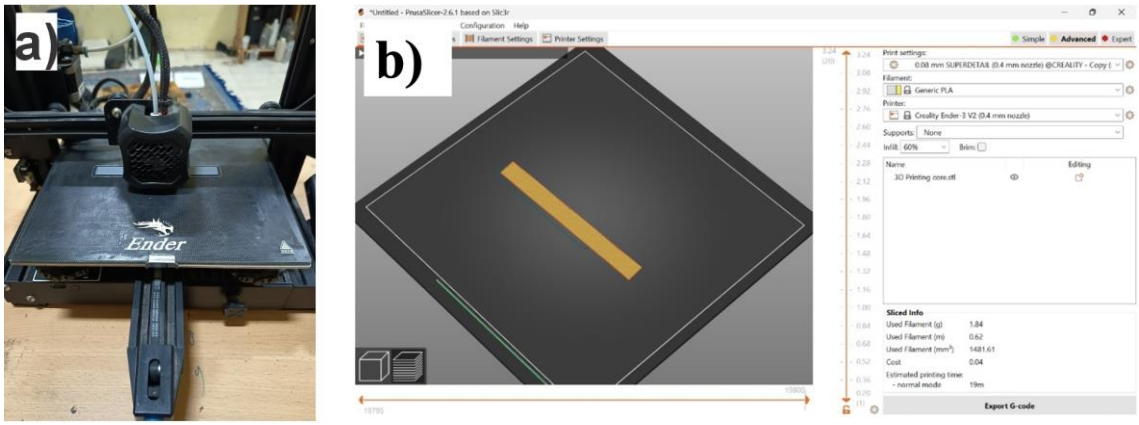

Figure 3. Additive manufacturing process (a) Fabrication process of the honeycomb core, (b) 3D printing parameter configuration

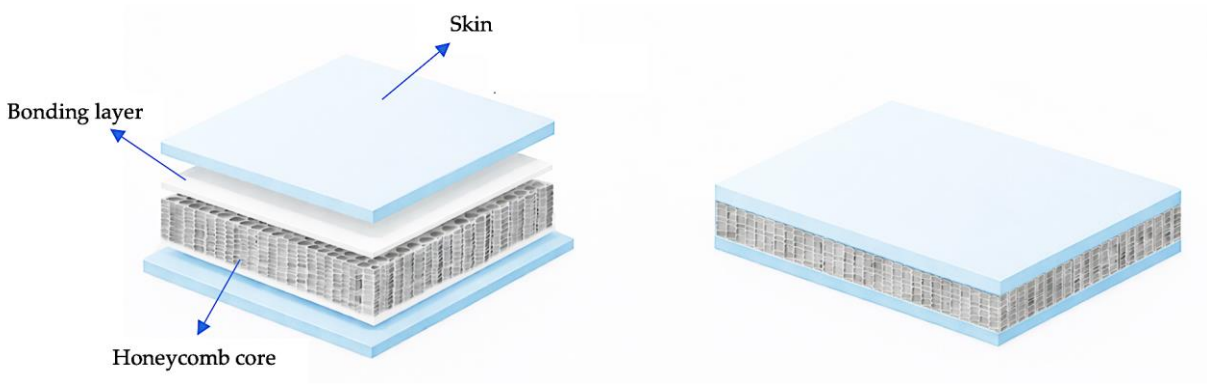

Figure 4. Configuration of the sandwich composite structure

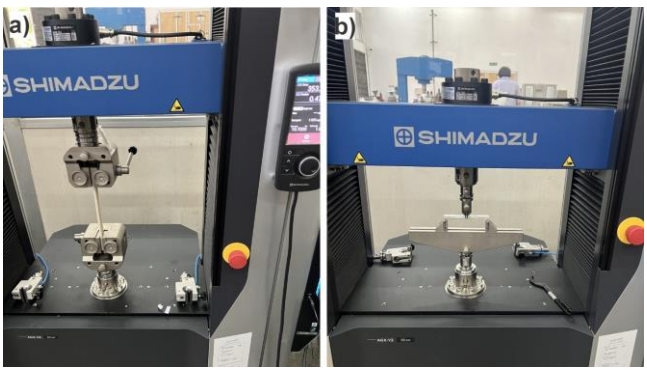

Figure 5. Mechanical testing of composites (a) Tensile testing, (b) Three-point bending testing

2.5 Scanning Electron Microscopy analysis

The surface morphology of the composite specimens was characterized using a Field-Emission Scanning Electron Microscope (JEOL JSM-IT700HR, Japan) operated at 10 kV.

2.6 Thermogravimetric Analysis

Thermogravimetric Analysis (TGA) was conducted to evaluate the effect of $CaCO_3$ volume fraction variation on several parameters, including thermal stability, decomposition temperature, mass loss behavior, and residue formation of the sandwich composite. This analysis aimed to identify the role of $CaCO_3$ as an inorganic filler in enhancing heat resistance and retarding the degradation rate of the sandwich composite

material. The test was performed using a Netzsch Simultaneous Thermal Analyzer (STA 449 F3 Jupiter). Measurements were carried out over a temperature range of 30 to 600 ℃ at a heating rate of 10 ℃/min under a nitrogen atmosphere.

3. RESULTS AND DISCUSSION

3.1 Tensile and flexural testing

The tensile test results of the sandwich composite specimens obtained using a UTM are presented in Figure 6. The results indicate that the addition of $CaCO_3$ powder significantly influences the tensile strength of the PLA honeycomb core sandwich composite with randomly oriented fiberglass skins. The tensile strength increased up to a filler content of 5 wt%, then declined as the $CaCO_3$ concentration increased to 10 wt% and 15 wt%. In the absence of filler (0 wt%), the sandwich composite exhibited a tensile strength of 48.61 MPa. This value increased to 49.082 MPa with the addition of 5 wt% $CaCO_3$, representing the highest tensile strength among all $CaCO_3$ variations. This improvement can be attributed to the role of $CaCO_3$ particles as reinforcing agents, which optimize load transfer and thereby minimize deformation under applied loading. When $CaCO_3$ particles are well dispersed within the epoxy matrix, part of the externally applied load can be sustained by the filler particles. Additionally, the presence of $CaCO_3$ can hinder interfacial slippage between the matrix and the fibers through a pinning mechanism. The filler also reduces stress concentration within the fibers during mechanical loading, thereby increasing the stress required to initiate failure in the fiberglass reinforcement. Consequently, a homogeneous dispersion of $CaCO_3$ results in a more uniform load distribution throughout the sandwich composite and enhances its overall mechanical performance. However, at higher filler contents of 10 wt% and 15 wt%, the tensile strength decreased to 45.625 MPa and 36.585 MPa, respectively. The increased $CaCO_3$ content may produce adverse effects due to excessive additive loading. At 10 wt%, particle agglomeration was observed within the epoxy resin, resulting in microdefects resembling cracks. Under external loading, stress concentrations tend to localize around these agglomerated regions, ultimately reducing the mechanical properties of the composite [27].

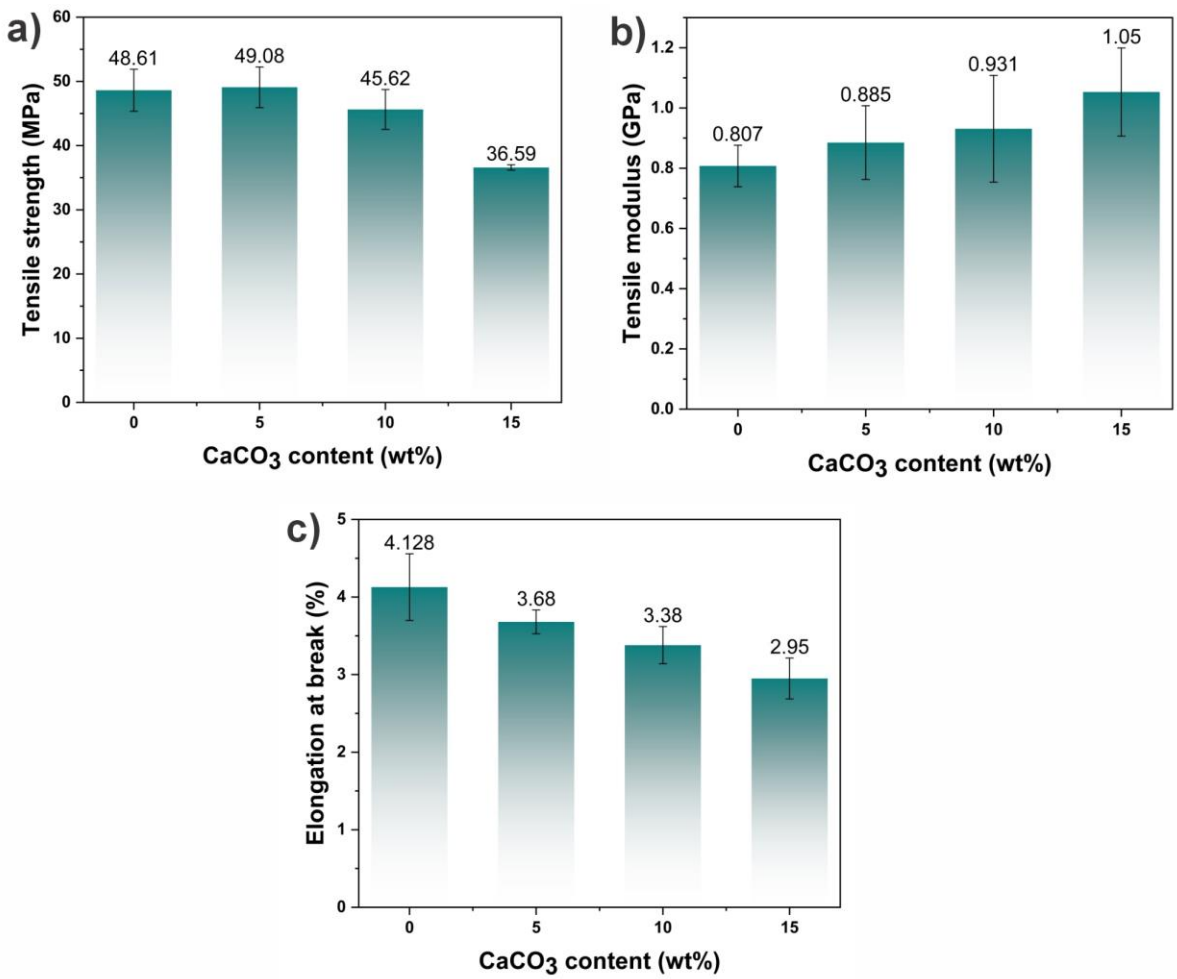

Figure 6. Tensile properties of sandwich composites (a) tensile strength, (b) tensile modulus, and (c) elongation at break

The flexural test results of the sandwich composite material (Figure 7) with varying $CaCO_3$ filler contents show higher flexural strength values compared to tensile strength. In the absence of filler (0 wt%), the sandwich composite exhibited a flexural strength of 76.486 MPa. This value increased to 78.647 MPa with the addition of 5 wt% $CaCO_3$. However, further increases in $CaCO_3$ content to 10 wt% and 15 wt% resulted in a decrease in flexural strength to 66.046 MPa and 43.432 MPa, respectively. During flexural loading, the specimen experiences compressive stress in the region above

the neutral axis and tensile stress in the region below the neutral axis. Under combined tensile–compressive stress conditions, the matrix's role becomes more dominant than under pure tensile loading. Consequently, matrix reinforcement through the incorporation of $CaCO_3$ powder is more effective in improving flexural strength [28-30]**.** The results indicate that increasing the $CaCO_3$ content enhances both the elastic and flexural modulus of the sandwich composite. The elastic modulus values at 0 wt%, 5 wt%, 10 wt%, and 15 wt% $CaCO_3$ were 0.807 GPa, 0.885 GPa, 0.931 GPa, and 1.053 GPa, respectively. Meanwhile, the corresponding flexural modulus values were 1.848 GPa, 2.008 GPa, 2.262 GPa, and 2.554 GPa. This improvement can be attributed to the dispersion of $CaCO_3$ particles within the epoxy matrix, which restricts polymer chain mobility and consequently increases material stiffness. Moreover, the intrinsic stiffness of $CaCO_3$ filler is higher than that of the epoxy matrix, leading to a significant enhancement in both tensile and flexural moduli. The filler also fills voids or pores within the matrix and improves interfacial adhesion by increasing the effective contact area between the constituents. In addition, the presence of $CaCO_3$ facilitates load transfer from the matrix, thereby contributing to the overall increase in the sandwich composite's modulus [27, 31].

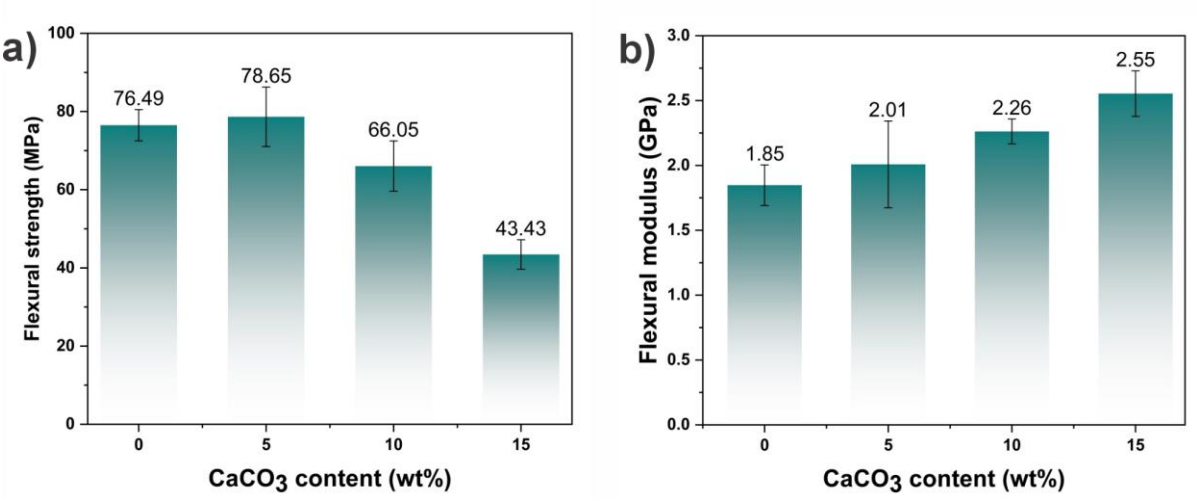

Figure 7. Flexural properties of sandwich composites (a) flexural strength, and (b) flexural modulus

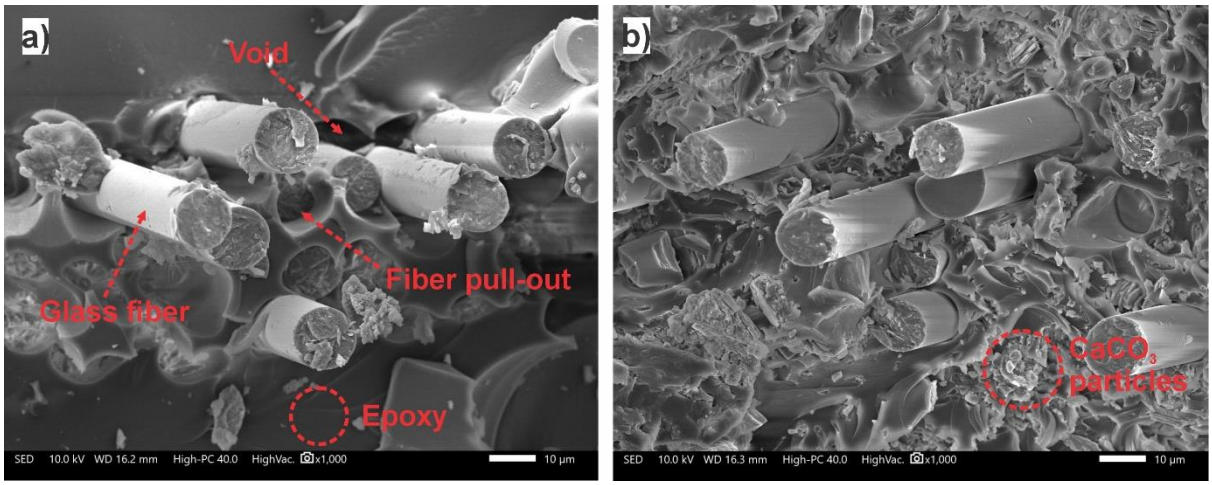

Figure 8. FE-SEM images of the sandwich composite samples (a) 0 wt% $CaCO_3$, and (b) 5 wt% $CaCO_3$

3.2 Morphological analysis

The morphological analysis results for the sandwich composite specimens after tensile and flexural testing are presented in Figures 8 and 9, respectively.

SEM observations of the sandwich composite specimen with 0 wt% $CaCO_3$, shown in Figure 8(a), reveal several fracture mechanisms during tensile testing, including fiber pull-out and interfacial debonding. Both failure mechanisms occurred at the interface between the glass fiber and the epoxy matrix. Fiber pull-out refers to the extraction of fibers from the matrix, whereas debonding occurs when the externally applied stress exceeds the interfacial bonding strength between the fiber and matrix [32, 33]. In the absence of $CaCO_3$ filler, the epoxy matrix serves as the sole load-transfer medium, transmitting stress to the glass fibers. The mismatch in elastic modulus between the glass fibers and the epoxy matrix leads to stress concentration at the fiber-matrix interface. Consequently, microcracks initiate and propagate along the fiber–matrix interface [34, 35]. This condition occurs more readily in the absence of $CaCO_3$ particles, which could otherwise enhance matrix–fiber interfacial bonding and improve interfacial adhesion [36, 37]. The debonding mechanism eventually progresses to fiber pull-out, in which the glass fibers are extracted from the matrix without fracturing under continued loading. Figure 8(a) clearly shows

extensive fiber pull-out traces, indicating weakened interfacial bonding and inefficient load transfer, ultimately leading to fiber extraction under increasing tensile load. Figure 8(b) presents the SEM image of the composite specimen containing 10 wt% $CaCO_3$, illustrating the dispersion of $CaCO_3$ particles within the epoxy matrix. The image shows that most glass fibers fractured rather than being pulled out, although limited fiber pull-out is still observed. This suggests that the addition of $CaCO_3$ restricts polymer chain mobility and enhances matrix cohesion, thereby requiring higher energy for crack initiation and propagation. $CaCO_3$ particles can also contribute to crack deflection and crack pinning mechanisms along the interface. However, particle agglomeration is also evident in the microstructure [38, 39], potentially forming localized stress-concentration zones and reducing mechanical strength. Agglomeration is a mechanism in which small particles cluster or form lumps into larger particle aggregates due to the presence of attractive forces between the particles. Regions surrounding the agglomerates may serve as crack-initiation sites due to non-uniform stress distribution, leading to localized stress accumulation. This condition facilitates the formation of microcracks and accelerates crack propagation. Furthermore, $CaCO_3$ agglomeration reduces the efficiency of load transfer from the matrix to the reinforcing fibers, thereby contributing to the reduction in tensile and flexural strength of the composite [27, 40].

Figure 9(a) shows the macroscopic fracture patterns after flexural testing of the sandwich composite specimen. For the 0 wt% $CaCO_3$ composition, the dominant failure mechanisms include fiber pull-out and delamination at both the upper and lower surfaces of the PLA honeycomb core. Delamination is a typical failure mechanism in layered materials such as sandwich composites, occurring when separation between the core and skin layers results from reduced interfacial bonding strength [37]. The macro image of the 5 wt% $CaCO_3$ specimen (Figure 9(b)) shows similar failure mechanisms, including fiber pull-out and delamination; however, delamination occurs only on one surface. Figures 9(c) and 9(d) exhibit more complex failure mechanisms, including fiber pull-out, delamination, voids, and porosity. Voids and porosity are formed by trapped air or gas during the hand lay-up fabrication process, commonly due to insufficient matrix mixing, non-uniform filler distribution, and excessively high resin viscosity [41, 42]. The presence of voids and porosity in the composite reduces tensile and flexural strength due to stress concentration around these cavities [43, 44].

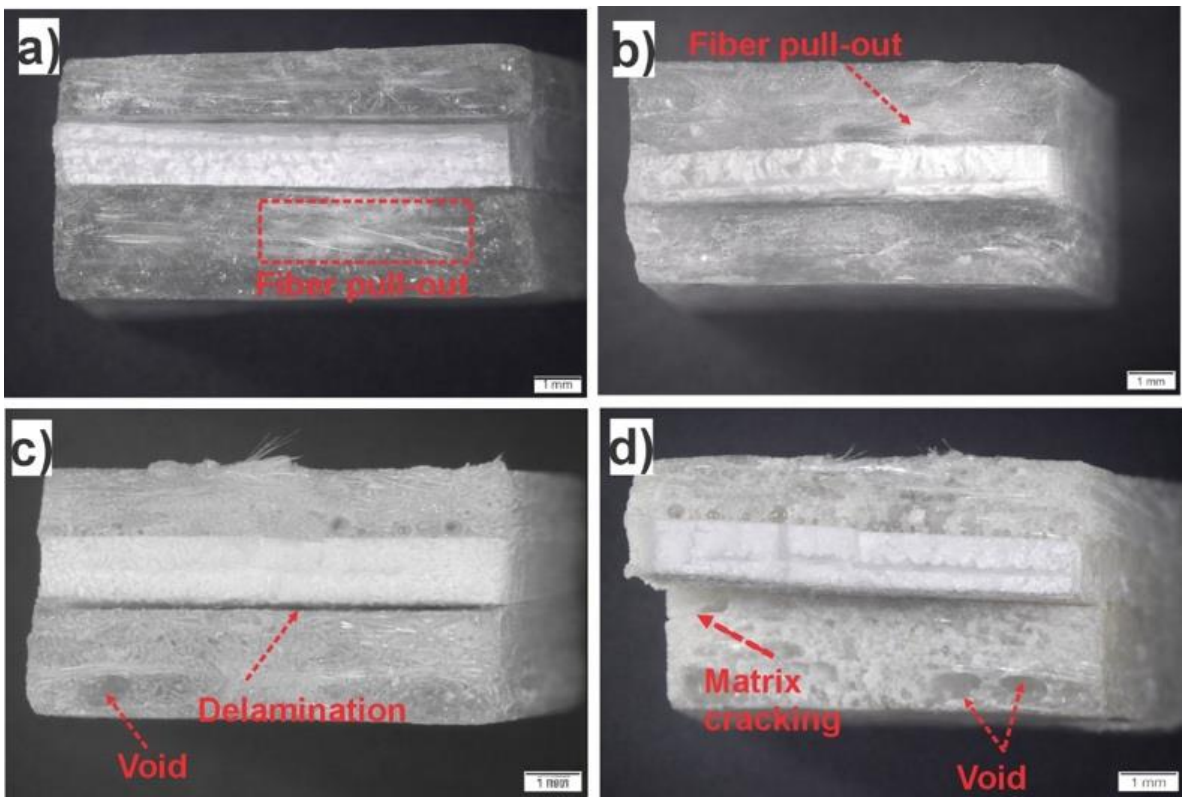

Figure 9. Macro images of the samples after flexural testing (a) 0 wt% $CaCO_3$, (b) 5 wt% $CaCO_3$, (c) 10 wt% $CaCO_3$, and (d) 15 wt% $CaCO_3$

3.3 Thermogravimetric Analysis

TGA is a thermal characterization technique used to monitor changes in material mass as a function of temperature or time. In this study, the analysis was conducted over a temperature range of 20 °C to 600 °C to evaluate the thermal stability of the sandwich composite and examine the effect of $CaCO_3$ filler addition on the material's degradation behavior. Figure 8 presents the thermogravimetric (TG) and derivative thermogravimetric (DTG) curves of the sandwich composite specimens. Table 2 summarizes the variations in specimen composition based on $CaCO_3$ content, along with the onset temperature (T_{onset}), the maximum decomposition temperature (T_{max}), and the residual mass ($W_{residue}$), as extracted from the data presented in Figure 10.

Figure 10(a) presents the TG curves illustrating the mass loss behavior of the sandwich composites with varying $CaCO_3$ weight fractions. All samples exhibit a similar trend, where the mass remains relatively stable up to approximately 200–250 °C. This indicates that no significant evaporation or

degradation occurs within this temperature range, except for the possible removal of residual moisture or minor volatile components. As the temperature increases to 300–400 °C, a substantial mass loss is observed for all specimens, corresponding to the primary degradation stage of the polymer matrix. Beyond 400 °C, differences in the residual mass among the samples become evident. The highest residual mass was recorded for the 15 wt% $CaCO_3$ specimen at 35.1%, followed by 10 wt% (32.5%), 5 wt% (30.3%), and the lowest value for 0 wt% $CaCO_3$ at 17.7%. This phenomenon indicates that incorporating $CaCO_3$ as an inorganic filler increases the final residual mass after thermal exposure. Consequently, composites containing $CaCO_3$ exhibit improved resistance to total thermal degradation compared to the unfilled composite [45, 46].

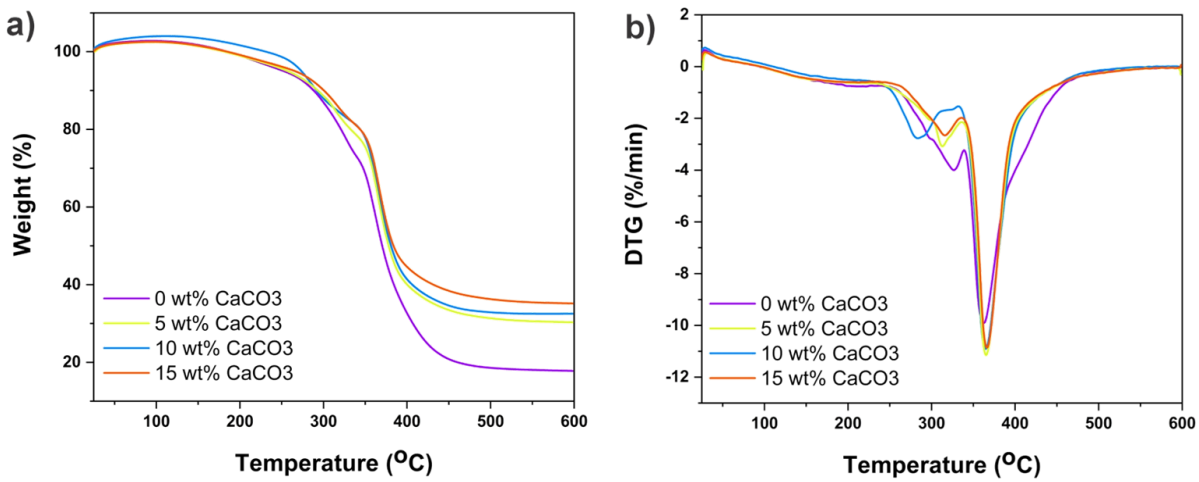

Figure 10. Thermal analysis of (a) Thermogravimetric Analysis (TGA), and (b) derivative thermogravimetric (DTG) curves

Table 2. Thermal Characteristics of Sandwich Composite

Samples	T_{onset} (°C)	T_{max} (°C)	$W_{residue}$ (%)
$CaCO_3$ 0 wt%	317.3	361.3	17.7
$CaCO_3$ 5 wt%	326.7	364.9	30.3
$CaCO_3$ 10 wt%	330.1	365.5	32.5
$CaCO_3$ 15 wt%	332.8	365.9	35.1

According to Table 2, the thermal parameters of the sandwich composites demonstrate an increasing trend in thermal stability with higher $CaCO_3$ content. The onset temperature (T_{onset}) increased significantly from 317.3 °C for the unfilled specimen to 332.8 °C for the 15 wt% $CaCO_3$ composite, indicating that $CaCO_3$ addition delays the initiation of thermal degradation. This finding is consistent with the DTG curves shown in Figure 10(b), where the initial degradation stage corresponds to polymer chain scission and loss of structural integrity. Meanwhile, the maximum degradation temperature (T_{max}) ranges from 361.3 °C to 365.9 °C. A slight increase in temperature in the filled composites suggests enhanced thermal resistance. This behavior is attributed to the inherently higher thermal stability of $CaCO_3$ compared to the polymer matrix, as it does not fully decompose within the tested temperature range [47, 48]. Furthermore, the presence of $CaCO_3$ may promote the formation of a more stable residual or char layer, which acts as a thermal barrier that reduces heat transfer and slows further degradation. The addition of $CaCO_3$ composition significantly increases the residual char content, as evidenced by the TGA results shown in Figure 10 and Table 2. An increase in $CaCO_3$ content in the sandwich composite material is directly proportional to the rise in $W_{residue}$, indicating the formation of a higher amount of thermal residue. Furthermore, the increase in T_{onset} and T_{max} suggests improved thermal stability of the material. Overall, these results indicate that the presence of $CaCO_3$ contributes to the formation of a protective residue that has the potential to inhibit heat transfer and slow down the degradation process. The increase in $W_{residue}$ reflects an enhancement in the thermal stability of the material with increasing $CaCO_3$ filler content [49, 50].

4. CONCLUSION

This study investigated the effect of incorporating inorganic $CaCO_3$ filler into 3D-printed PLA honeycomb core sandwich composites with fiberglass skins on their mechanical properties and thermal stability, evaluated through tensile, flexural, and TGA. The main findings can be summarized as follows:

1. The addition of inorganic $CaCO_3$ filler significantly influenced the mechanical properties of the 3D-printed PLA honeycomb core sandwich composites with fiberglass skins. The highest tensile and flexural strengths were achieved at 5 wt% $CaCO_3$, with values of 49.082 MPa and 78.647 MPa, respectively. However, both tensile and flexural strengths decreased at higher filler contents of 10 wt% and 15 wt%, primarily due to particle agglomeration within the matrix, which reduced the mechanical performance of the sandwich composite.
2. The elastic modulus and flexural modulus increased with increasing $CaCO_3$ content in the epoxy matrix. This improvement is attributed to the higher intrinsic stiffness of $CaCO_3$ relative to that of the epoxy matrix. Additionally, the dispersion of $CaCO_3$ particles enhances load distribution within the matrix, contributing to the observed increase in both elastic and flexural moduli of the sandwich composite.
3. SEM morphological analysis of the sandwich composite without $CaCO_3$ (0 wt%) revealed fiber pull-out and interfacial debonding mechanisms. In contrast, the specimen containing 10 wt% $CaCO_3$ exhibited fiber pull-out accompanied by particle agglomeration, which may

lead to stress concentration and reduced mechanical strength. Macro-fracture observations showed fiber pull-out and delamination in all specimens. However, voids and porosity were observed in the 10 wt% and 15 wt% $CaCO_3$ compositions, which contributed to stress concentration and subsequent reductions in tensile and flexural strength.

4. TGA demonstrated that the addition of $CaCO_3$ filler increased both the onset temperature (T_{onset}) and the maximum degradation temperature (T_{max}). Higher $CaCO_3$ content delayed the initiation of thermal degradation and improved resistance to thermal exposure. The presence of $CaCO_3$ promotes the formation of a more stable char layer, which acts as a thermal barrier and retards further degradation. Consequently, the residual mass ($W_{residue}$) increased with increasing $CaCO_3$ content.

ACKNOWLEDGMENT

The authors would like to express their sincere gratitude to the Ministry of Higher Education, Science, and Technology of the Republic of Indonesia for the financial support under Contract No. 120/C3/DT.05.00/PL/2025, as well as for the guidance provided throughout the implementation of this research. The authors also gratefully acknowledge Universitas Gadjah Mada, Yogyakarta, for providing the facilities that supported the completion of this study.

REFERENCES

[1] Bacciaglia, A., Ceruti, A., Liverani, A. (2022). Towards large parts manufacturing in additive technologies for aerospace and automotive applications. Procedia Computer Science, 200: 1113-1124. https://doi.org/10.1016/j.procs.2022.01.311

[2] Pasco, J., Lei, Z., Aranas Jr, C. (2022). Additive manufacturing in off-site construction: Review and future directions. Buildings, 12(1): 53. https://doi.org/10.3390/buildings12010053

[3] Bayat, M., Kharel, S., Li, J. (2025). On the effects of additive manufacturing on affordable housing development: A review. Sustainability, 17(12): 5328. https://doi.org/10.3390/su17125328

[4] Tilford, T., Stoyanov, S., Braun, J., Janhsen, J.C., Burgard, M., Birch, R., Bailey, C. (2018). Design, manufacture and test for reliable 3D printed electronics packaging. Microelectronics Reliability, 85: 109-117. https://doi.org/10.1016/j.microrel.2018.04.008

[5] Omiyale, B.O., Farayibi, P.K. (2020). Additive manufacturing in the oil and gas industries: A review. Analecta Technica Szegedinensia, 14(1): 9-18. https://doi.org/10.14232/analecta.2020.1.9-18

[6] Verhoef, L.A., Budde, B.W., Chockalingam, C., Nodar, B.G., van Wijk, A.J. (2018). The effect of additive manufacturing on global energy demand: An assessment using a bottom-up approach. Energy Policy, 112: 349-360. https://doi.org/10.1016/j.enpol.2017.10.034

[7] Hassanpour Roudbeneh, F., Liaghat, G., Sabouri, H., Hadavinia, H. (2020). High-velocity impact loading in honeycomb sandwich panels reinforced with polymer foam: A numerical approach study. Iranian Polymer Journal, 29(8): 707-721. https://doi.org/10.1007/s13726-020-00833-5

[8] Výtisk, J., Kočí, V., Honus, S., Vrtek, M. (2019). Current options in the life cycle assessment of additive manufacturing products. Open Engineering, 9(1): 674-682. https://doi.org/10.1515/eng-2019-0073

[9] Manalo, A.C. (2013). Behaviour of fibre composite sandwich structures under short and asymmetrical beam shear tests. Composite Structures, 99: 339-349. https://doi.org/10.1016/j.compstruct.2012.12.010

[10] Turner, A.J., Al Rifaie, M., Mian, A., Srinivasan, R. (2018). Low-velocity impact behavior of sandwich structures with additively manufactured polymer lattice cores. Journal of Materials Engineering and Performance, 27(5): 2505-2512. https://doi.org/10.1007/s11665-018-3322-x

[11] Kumar, A., Chanda, A. K., Angra, S. (2021). Analysis of effects of varying face sheet thickness on different properties of composite sandwich structure. Materials Today: Proceedings, 38: 116-121. https://doi.org/10.1016/j.matpr.2020.06.114

[12] Tanniru, M., Misra, R.D.K. (2005). On enhanced impact strength of calcium carbonate-reinforced high-density polyethylene composites. Materials Science and Engineering: A, 405(1-2): 178-193. https://doi.org/10.1016/j.msea.2005.05.083

[13] Jang, W.C., Roh, H.D. (2025). Sandwich composites manufacturing: A review of materials, methods, applications and challenges. International Journal of Precision Engineering and Manufacturing, 26(8): 2093-2109. https://doi.org/10.1007/s12541-025-01285-8

[14] Chen, Q., Linghu, T., Gao, Y., Wang, Z., Liu, Y., Du, R., Zhao, G. (2017). Mechanical properties in glass fiber PVC-foam sandwich structures from different chopped fiber interfacial reinforcement through vacuum-assisted resin transfer molding (VARTM) processing. Composites Science and Technology, 144: 202-207. https://doi.org/10.1016/j.compscitech.2017.03.033

[15] Widodo, R.D., Nuryanta, M.I., Handayani, P.A., Ichwan, R., Zainudin, E.S., Muflikhun, M.A. (2026). Sustainable hybrid laminated composites reinforced with bamboo, flex banner, and glass fibers: Impact of CaCO3 filler on mechanical properties. Polymers, 18(2): 275. https://doi.org/10.3390/polym18020275

[16] Deswita, D., Yusmaniar, Y., Sulungbudi, G.T., Karo, A.K., Sudirman, S. (2022). Influence of nanoparticle CaCO3 addition to the physical and mechanical properties of polypropylene-CaCO3 composite. Journal of Fibers and Polymer Composites, 1(1): 43-51. https://doi.org/10.55043/jfpc.v1i1.34

[17] Sun, Y., Zhang, P., Guo, W., Bao, J., Qu, C. (2020). Effect of Nano-CaCO3 on the mechanical properties and durability of concrete incorporating fly ash. Advances in Materials Science and Engineering, 2020(1): 7365862. https://doi.org/10.1155/2020/7365862

[18] Tang, H., Hu, X. (2023). The effect of calcium carbonate whiskers on the thermal stability of environmentally friendly and energy-saving building composites. Journal of Physics: Conference Series, 2553(1): 012027. https://doi.org/10.1088/1742-6596/2553/1/012027

[19] Feng, D., Loi, G., Aymerich, F. (2022). A numerical and experimental investigation into the impact response of Sandwich composites under different boundary conditions. Journal of Composites Science, 6(3): 88.

https://doi.org/10.3390/jcs6030088
[20] Hakamy, A. (2020). Effect of CaCO3 nanoparticles on the microstructure and fracture toughness of ceramic nanocomposites. Journal of Taibah University for Science, 14(1): 1201-1207. https://doi.org/10.1080/16583655.2020.1809840
[21] Stambouli, M., Chaouch, W., Gargoubi, S., Zouari, R., Msahli, S. (2023). Effect of calcium carbonate particle size and content on the thermal properties of PVC foamed layer used for coated textiles. Turkish Journal of Chemistry, 47(1): 40-46. https://doi.org/10.55730/1300-0527.3514
[22] Bakly, N.S., Al-Mutairi, N.H., Layla, A.A., Almaamori, M.H. (2023). Investigate the effect of temperature change on the properties of the PP/CaCO3 composites: A comparative study. Al-Mustaqbal Journal of Sustainability in Engineering Sciences, 1(2): 1. https://doi.org/10.62723/2959-5932.1000
[23] Budiyantoro, C., Sosiati, H., Kamiel, B.P., Fikri, M.L.S. (2018). The effect of CaCO3 filler component on mechanical properties of polypropylene. IOP Conference Series: Materials Science and Engineering, 432(1): 012043. https://doi.org/10.1088/1757-899X/432/1/012043
[24] Malak, S.A. (2021). Tensile stress strain model of polyvinyl chloride/calcium carbonate (PVC/CaCO3) nanocomposite plank. Results in Materials, 10: 100193. https://doi.org/10.1016/j.rinma.2021.100193
[25] Peng, Y., Musah, M., Via, B., Wang, X. (2021). Calcium carbonate particles filled homopolymer polypropylene at different loading levels: Mechanical properties characterization and materials failure analysis. Journal of Composites Science, 5(11): 302. https://doi.org/10.3390/jcs5110302
[26] Bodaghi, M., Serjouei, A., Zolfagharian, A., Fotouhi, M., Rahman, H., Durand, D. (2020). Reversible energy absorbing meta-sandwiches by FDM 4D printing. International Journal of Mechanical Sciences, 173: 105451. https://doi.org/10.1016/j.ijmecsci.2020.105451
[27] Abdi, A., Eslami-Farsani, R., Khosravi, H. (2018). Evaluating the mechanical behavior of basalt fibers/epoxy composites containing surface-modified CaCO3 nanoparticles. Fibers and Polymers, 19(3): 635-640. https://doi.org/10.1007/s12221-018-7755-x
[28] Eskizeybek, V., Ulus, H., Kaybal, H.B., Şahin, Ö.S., Avcı, A. (2018). Static and dynamic mechanical responses of CaCO3 nanoparticle modified epoxy/carbon fiber nanocomposites. Composites Part B: Engineering, 140: 223-231. https://doi.org/10.1016/j.compositesb.2017.12.013
[29] Yang, G., Heo, Y.J., Park, S.J. (2019). Effect of morphology of calcium carbonate on toughness behavior and thermal stability of epoxy-based composites. Processes, 7(4): 178. https://doi.org/10.3390/pr7040178
[30] Sugiman, S., Setyawan, P.D., Maryudi, M., Madnasri, S. (2021). Water absorption, tensile, flexural and impact properties of aged bamboo fibre/nano CaCO3-modified unsaturated polyester composites. Journal of Applied Science and Engineering, 24(2): 239-251. http://doi.org/10.6180/jase.202104_24(2).0013
[31] Vijaya Rajan, V., Shanmugam, M., Santhanam, V., Ramkumar, S. (2020). Effect of CaCO3 particulate filler on the mechanical properties of surface modified coir fibre/epoxy composite. IOP Conference Series: Materials Science and Engineering, 988(1): 012046. http://doi.org/10.1088/1757-899X/988/1/012046
[32] Chang, W.X., Qing, H., Gao, C.F. (2016). A new theoretical model of the quasistatic single-fiber pull-out problem: A rate-dependent interfacial bond strength. Mechanics of Materials, 94: 132-141. https://doi.org/10.1016/j.mechmat.2015.12.001
[33] Zhang, H.P., Han, W., Tavakoli, J., Zhang, Y.P., et al. (2019). Understanding interfacial interactions of polydopamine and glass fiber and their enhancement mechanisms in epoxy-based laminates. Composites Part A: Applied Science and Manufacturing, 116: 62-71. https://doi.org/10.1016/j.compositesa.2018.10.024
[34] Wang, X., Li, H., Camilleri, D., Surnam, B.Y.R., et al. (2025). Analysis of interfacial properties in flax yarn-reinforced epoxy resin composites. Fibers, 13(9): 118. https://doi.org/10.3390/fib13090118
[35] Xu, P., Yu, Y., Liu, D., He, M., Li, G., Yang, X. (2018). Enhanced interfacial and mechanical properties of high-modulus carbon fiber composites: Establishing modulus intermediate layer between fiber and matrix based on tailored-modulus epoxy. Composites Science and Technology, 163: 26-33. https://doi.org/10.1016/j.compscitech.2018.05.009
[36] Shahbakhsh, S., Tohidlou, E., Khosravi, H. (2020). Influence of modified carbonate calcium nanoparticles on the mechanical properties of carbon fiber/epoxy composites. The Journal of the Textile Institute, 111(4): 550-554. https://doi.org/10.1080/00405000.2019.1651155
[37] Nekhamanurak, B., Patanathabutr, P., Hongsriphan, N. (2014). The influence of micro-/nano-CaCO3 on thermal stability and melt rheology behavior of poly (lactic acid). Energy Procedia, 56: 118-128. https://doi.org/10.1016/j.egypro.2014.07.139
[38] Sosiati, H., Utomo, C.T., Setiono, I., Budiyantoro, C. (2020). Effect of CaCO3 particles size and content on impact strength of kenaf/CaCO3/epoxy resin hybrid composites. Indonesian Journal of Applied Physics, 10(1): 24-31. https://doi.org/10.13057/ijap.v10i01.37748
[39] Huang, T., Bobyr, M. (2023). A review of delamination damage of composite materials. Journal of composites science, 7(11): 468. https://doi.org/10.3390/jcs7110468
[40] Tochaikul, G., Tanadchangsaeng, N., Panaksri, A., Moonkum, N. (2025). Enhancing radiation shielding capabilities with epoxy-resin composites reinforced with coral-derived calcium carbonate fillers. Polymers, 17(1): 113. https://doi.org/10.3390/polym17010113
[41] Gagauz, I., Kawashita, L.F., Hallett, S.R. (2017). Understanding the effect of void morphology and characteristics on laminate mechanical properties. In 21st International Conference on Composite Materials, Xi'an, China, pp. 1-8.
[42] Mehdikhani, M., Gorbatikh, L., Verpoest, I., Lomov, S.V. (2019). Voids in fiber-reinforced polymer composites: A review on their formation, characteristics, and effects on mechanical performance. Journal of Composite Materials, 53(12): 1579-1669. https://doi.org/10.1177/0021998318772152
[43] Okolie, O., Latto, J., Faisal, N., Jamieson, H., Mukherji, A., Njuguna, J. (2023). Manufacturing defects in thermoplastic composite pipes and their effect on the in-situ performance of thermoplastic composite pipes in oil

and gas applications. Applied composite materials, 30(1): 231-306. https://doi.org/10.1007/s10443-022-10066-9

[44] Vajari, D.A., González, C., Llorca, J., Legarth, B.N. (2014). A numerical study of the influence of microvoids in the transverse mechanical response of unidirectional composites. Composites Science and Technology, 97: 46-54. https://doi.org/10.1016/j.compscitech.2014.04.004

[45] Liu, Z., Meng, F., Tang, X., Su, C., Mu, Q., Ju, G. (2023). Research on properties of PBAT/CaCO3 composite films modified with titanate coupling agent. Polymers, 15(10): 2379.

[46] Tuen, B.S., Hassan, A., Abu Bakar, A. (2012). Thermal properties and processability of talc-and calcium carbonate-filled poly(vinyl chloride) hybrid composites. Journal of Vinyl and Additive Technology, 18(2): 87-94. https://doi.org/10.1002/vnl.20312

[47] Issakah, O., Kayaba, A.M., Fiagbe, Y., Akromah, S., Kpare, J.Y., Asare, E.K.A. (2025). Effect of partial replacement of CaCO3 with palm kernel shell particles on the mechanical properties of PKS/CaCO3/HDPE hybrid composites. Results in Materials, 25: 100668. https://doi.org/10.1016/j.rinma.2025.100668

[48] Sahebian, S., Mosavian, M.T.H. (2019). Thermal stability of $CaCO_3$/polyethylene (PE) nanocomposites. Polymers and Polymer Composites, 27(7): 371-382. https://doi.org/10.1177/0967391119845994

[49] Tao, Y., Li, P., Cai, L., Shi, S.Q. (2019). Flammability and mechanical properties of composites fabricated with CaCO3-filled pine flakes and Phenol Formaldehyde resin. Composites Part B: Engineering, 167: 1-6. https://doi.org/10.1016/j.compositesb.2018.12.005

[50] Shao, P., Xu, P., Zhang, L., Xue, Y., Zhao, X., Li, Z., Li, Q. (2019). Non-chloride in situ preparation of nano-cuprous oxide and its effect on heat resistance and combustion properties of calcium alginate. Polymers, 11(11): 1760. https://doi.org/10.3390/polym11111760